www.lajss.org
Latin American Journal of Solids and Structures 3 (2006) 245–261

Stability and nonlinear dynamic behaviour of cross-ply laminated heated cylindrical shells

B. P. Patel*, S. Singh and Y. Nath

Department of Applied Mechanics, Indian Institute of Technology Delhi, New Delhi 110 016, India

Abstract

The stability of postbuckled equilibrium configurations and the nonlinear dynamic characteristics of cross-ply laminated heated cylindrical shells are investigated employing semi-analytical shell finite element. The presence of asymmetric perturbation in the form of small magnitude load spatially proportional to the linear buckling mode shape is considered to initiate the bifurcation of the shell deformation from axisymmetric mode to asymmetric one. The frequencies of small oscillations about equilibrium configuration are obtained by solving the eigenvalue problem formulated using tangent stiffness matrix of the converged equilibrium configuration and mass matrix. The study reveals that the prediction of the postbuckling equilibrium configuration from nonlinear static analysis depends on the nature (longitudinally symmetric/antisymmetric) of initial disturbance. The longitudinally antisymmetric postbuckled equilibrium configuration is stable whereas the longitudinally symmetric one is unstable. The nonlinear dynamic response shows that the shell with longitudinally symmetric disturbance jumps from symmetric mode to antisymmetric mode and the predicted equilibrium configuration is of antisymmetric nature irrespective of the type of initial disturbance. The nonlinear forced dynamic response of the heated shell in the prebuckling region differs significantly from that in the postbuckling region.

Keywords: dynamics, stability, cylindrical shell, cross-ply, thermal, postbuckling, semi-analytical finite element

1 Introduction

The advances in composite technology have lead to the increasing application of laminated structures tailored for the required performance as load-bearing members in the design of more and more sophisticated futuristic structural systems such as in space shuttles, supersonic/hypersonic vehicles, rockets, missiles, nuclear reactors, engine components etc. These structures may often be subjected to dynamic loading environment coupled with the continuous and/or sudden exposure to elevated temperature. In view of the utilization of postbuckling strength, aero-space structures may be permitted to undergo elastic buckling and operate in postbuckling region. The structures in their buckled state may be expected to survive under dynamic disturbances.

*Corresp. author Email: badripatel@hotmail.com Received 28 Mar 2006; In revised form 11 Aug 2006

The thermo-mechanical loading environment may cause instability and/or dynamic response resulting in transverse deflections of the order of shell thickness or even higher necessitating the inclusion of geometric nonlinearity for the adequate analysis. The induced thermal state of stress in the pre-buckling and post-buckled configurations may significantly affect the vibration characteristics. Further, the frequency characteristics of small amplitude vibrations about the post-buckled configuration as the mean configuration reveal the stability/instability of post-buckling equilibrium path. Therefore, the study of vibration characteristics of thermally stressed composite laminated structures in the pre-/post-buckling regions gains importance.

Few studies on the free vibration characteristics of laminated plates subjected to thermal loading in the pre- and post-buckling configuration have been carried out [5, 8, 12–14]. The vibration frequencies corresponding to first three modes of thermally stressed laminated plates in pre- and post-buckled configurations have been analyzed using first order shear deformation theory and finite element approach by Lee and Lee [8]. The authors [8] have carried out the vibration analysis using the tangent stiffness obtained from the converged nonlinear static analysis. Similar study is carried out by Girish and Ramachandra [5] using higher-order shear deformation theory and adopting the multi-term Galerkin's approach. The vibration characteristics of piezolaminated composite plates subjected to thermopiezoelectric loads are studied [12] employing finite element based on layerwise theory in pre- and post-buckled regions. The composite laminated plates embedded with the shape memory alloy fibers are investigated [13, 14] for their free vibration behaviour in the pre- and post-buckled equilibrium configurations.

The investigation of vibration characteristics of thermally buckled composite laminated shell panels has received attention of few researchers [9–11] wherein the cylindrical panels are analyzed for their frequencies of free flexural oscillations about the deformed static equilibrium configuration. The single term Galerkin's approach is employed in Refs. [9, 10] and finite element based on layerwise theory in Ref. [11]. The variation of asymmetric mode free vibration frequencies of laminated cylindrical shells with temperature rise is studied in Refs. [3, 4] wherein the results are limited to pre-buckling configuration derived from linear static analysis.

To the best of the authors' knowledge, the studies on the vibration characteristics of laminated heated cylindrical shells in the post-buckled regions and the investigation on the stability of post-buckling equilibrium configurations through dynamic analysis (eigenvalue and response approaches) are not available in the open literature. Furthermore, the behaviour of the circumferentially closed shells especially undergoing large deformation is significantly different from the panels/plates.

Therefore, in the present work, the stability of postbuckled equilibrium configurations and nonlinear dynamic characteristics of cross-ply laminated heated cylindrical shells are studied employing semi-analytical shell finite element used recently for thermoelastic buckling/postbuckling studies of laminated conical/cylindrical shells [15, 16]. Geometric nonlinearity of von K*árm*án type is incorporated in the formulation. The presence of asymmetric perturbation in the form of small magnitude load spatially proportional to the linear buckling mode shape is considered to initiate the bifurcation of the shell from axisymmetric mode to asymmetric one. The

frequencies of small oscillations about equilibrium configuration corresponding to each temperature/displacement increment are obtained by solving the eigenvalue problem formulated using tangent stiffness matrix of the converged configuration and mass matrix. The nonlinear dynamic response of the heated shell in prebuckling and postbuckling regions is carried out incorporating a small amount of proportional damping. The damping is introduced for two purposes: firstly to incorporate the realistic situation wherin small amount of damping is always present and secondly in order to facilitate the convergence to a new stable state after jump.

2 Formulation

A laminated composite circular cylindrical shell is considered with the co-ordinates s, θ and z along the meridional, circumferential and radial/thickness directions, respectively. The displacements u, v, w at a point (s, θ, z) from the median surface are expressed as functions of middle-surface displacements u_0, v_0 and w_0, and independent rotations β_s and β_θ of the meridional and hoop sections, respectively, as

$$\begin{aligned} u(s,\theta,z,t) &= u_0(s,\theta,t) + z\beta_s(s,\theta,t) \\ v(s,\theta,z,t) &= v_0(s,\theta,t) + z\beta_\theta(s,\theta,t) \\ w(s,\theta,z,t) &= w_0(s,\theta,t) \end{aligned} \tag{1}$$

where t is the time.

Using the semi-analytical approach, u_0, v_0, w_0, β_s, and β_θ are represented by a Fourier series in the circumferential co-ordinate θ. For the nth harmonic, these can written as [15, 16]

$$\begin{aligned} u_0(s,\theta,t) &= u_0^0(s,t) + \sum_{i=1}^{M_1}\{u_0^{c_i}(s,t)cos(in\theta) + u_0^{s_i}(s,t)sin(in\theta)\} \\ v_0(s,\theta,t) &= v_0^0(s,t) + \sum_{i=1}^{M_1}\{v_0^{c_i}(s,t)cos(in\theta) + v_0^{s_i}(s,t)sin(in\theta)\} \\ w_0(s,\theta,t) &= w_0^0(s,t) + \sum_{i=1}^{M_2}\{w_0^{c_i}(s,t)cos(in\theta) + w_0^{s_i}(s,t)sin(in\theta)\} \\ \beta_s(s,\theta,t) &= \beta_s^0(s,t) + \sum_{i=1}^{M_2}\{\beta_s^{c_i}(s,t)cos(in\theta) + \beta_s^{s_i}(s,t)sin(in\theta)\} \\ \beta_\theta(s,\theta,t) &= \beta_\theta^0(s,t) + \sum_{i=1}^{M_2}\{\beta_\theta^{c_i}(s,t)cos(in\theta) + \beta_\theta^{s_i}(s,t)sin(in\theta)\} \end{aligned} \tag{2}$$

where superscript 0 refers to the axisymmetric components of the displacement field variables, and c_i and s_i refer to the asymmetric components of the field variables having circumferential

variation proportional to $cos(in\theta)$ and $sin(in\theta)$, respectively. The number of terms M_1 in the approximation of variables (u_0, v_0) is in general twice compared to M_2 in $(w_0, \beta_s, \beta_\theta)$ for the converged solution.

Using von Kármán's assumption for moderately large deformation, Green's strains can be written in terms of middle surface deformations as,

$$\{\varepsilon\} = \left\{ \begin{array}{c} \varepsilon_p^L \\ 0 \end{array} \right\} + \left\{ \begin{array}{c} z\varepsilon_b \\ \varepsilon_s \end{array} \right\} + \left\{ \begin{array}{c} \varepsilon_p^{NL} \\ 0 \end{array} \right\} \tag{3}$$

where, the membrane strains $\{\varepsilon_p^L\}$, bending strains $\{\varepsilon_b\}$, transverse shear strains $\{\varepsilon_s\}$ and nonlinear in-plane strains $\{\varepsilon_p^{NL}\}$ in the Eq. (3) are written as [7]

$$\{\varepsilon_p^L\} = \left\{ \begin{array}{c} \frac{\partial u_0}{\partial s} \\ \frac{\partial v_0}{r\partial\theta} + \frac{w_0}{r} \\ \frac{\partial u_0}{r\partial\theta} + \frac{\partial v_0}{\partial s} \end{array} \right\}; \qquad \{\varepsilon_b\} = \left\{ \begin{array}{c} \frac{\partial \beta_s}{\partial s} \\ \frac{\partial \beta_\theta}{r\partial\theta} \\ \frac{\partial \beta_s}{r\partial\theta} + \frac{\partial \beta_\theta}{\partial s} \end{array} \right\};$$

$$\{\varepsilon_s\} = \left\{ \begin{array}{c} \beta_s + \frac{\partial w_0}{\partial s} \\ \beta_\theta + \frac{\partial w_0}{r\partial\theta} - \frac{v_0}{r} \end{array} \right\}; \qquad \{\varepsilon_p^{NL}\} = \left\{ \begin{array}{c} \frac{1}{2}(\frac{\partial w_0}{\partial s})^2 \\ \frac{1}{2}(\frac{\partial w_0}{r\partial\theta})^2 \\ \frac{\partial w_0}{\partial s}\frac{\partial w_0}{r\partial\theta} \end{array} \right\} \tag{4}$$

where r is the radius of the shell.

If $\{N\}$ represents the stress resultants $(N_{ss},\ N_{\theta\theta},\ N_{s\theta})$ and $\{M\}$ the moment resultants $(M_{ss},\ M_{\theta\theta},\ M_{s\theta})$, one can relate these to membrane strains $\{\varepsilon_p\}(= \{\varepsilon_p^L\} + \{\varepsilon_p^{NL}\})$ and bending strains $\{\varepsilon_b\}$ through the constitutive relations as

$$\left\{ \begin{array}{c} \{N\} \\ \{M\} \end{array} \right\} = \left[\begin{array}{cc} [A] & [B] \\ [B] & [D] \end{array} \right] \left\{ \begin{array}{c} \{\varepsilon_p\} \\ \{\varepsilon_b\} \end{array} \right\} - \left\{ \begin{array}{c} \{\bar{N}\} \\ \{\bar{M}\} \end{array} \right\} \tag{5}$$

where $[A]$, $[D]$ and $[B]$ are extensional, bending and bending-extensional coupling stiffness coefficients matrices of the composite laminate. $\{\bar{N}\}$ and $\{\bar{M}\}$ are the thermal stress and moment resultants, respectively.

Similarly, the transverse shear stress resultants $\{Q\}$ representing the quantities $(Q_{sz}, Q_{\theta z})$ are related to the transverse shear strains $\{\varepsilon_s\}$ through the constitutive relation as

$$\{Q\} = [E]\{\varepsilon_s\} \tag{6}$$

where $[E]$ is the transverse shear stiffness coefficients matrix of the laminate.

For a laminated shell of thickness h, consisting of N layers with stacking angles $\theta_i (i = 1, ..., N)$ and layer thicknesses $h_i (i = 1, ..., N)$, the necessary expressions to compute the stiffness coefficients and thermal stress/moment resultants, available in the literature [6] are used here.

The potential energy functional $U_1(\delta)$ (due to strain energy and transverse load) is given by,

$$U_1(\delta) = \frac{1}{2}\int_A \left[\left\{ \begin{array}{c} \varepsilon_p \\ \varepsilon_b \end{array} \right\}^T \left[\begin{array}{cc} [A] & [B] \\ [B] & [D] \end{array} \right] \left\{ \begin{array}{c} \varepsilon_p \\ \varepsilon_b \end{array} \right\} + \{\varepsilon_s\}^T[E]\{\varepsilon_s\} - \left\{ \begin{array}{c} \varepsilon_p \\ \varepsilon_b \end{array} \right\}^T \left\{ \begin{array}{c} \bar{N} \\ \bar{M} \end{array} \right\} \right] dA - \int_A q w_0 dA \tag{7}$$

where δ is the vector of degrees of freedom associated to the displacement field in a finite element discretisation and q is the applied pressure load.

The potential energy $U_2(\delta)$ due to initial state of in-plane stress resultants $\{N^0\} = \{N^0_{ss}\ N^0_{\theta\theta}\ N^0_{s\theta}\}^T$ is written as

$$U_2(\delta) = \int_A \{\varepsilon_p^{NL}\}^T\{N^0\} dA \tag{8}$$

Following the procedure given in the work of Rajsekaran and Murray [17], the total potential energy functional $U(\delta)[= U_1(\delta) + U_2(\delta)]$ can be expressed as

$$U(\delta) = \{\delta\}^T[\frac{1}{2}[[K] - [K_{\Delta T}] + [K_G]] + \frac{1}{6}[N_1(\delta)] + \frac{1}{12}[N_2(\delta)]]\{\delta\} - \{\delta\}^T\{F_M\} - \{\delta\}^T\{F_T\} \tag{9}$$

where $[K]$ is the linear stiffness matrix, $[N_1]$ and $[N_2]$ are nonlinear stiffness matrices linearly and quadratically dependent on the field variables, respectively. $[K_{\Delta T}]$ and $[K_G]$ are the geometric stiffness matrices due to thermal and initial stress resultants. $\{F_M\}$ and $\{F_T\}$ are mechanical and thermal load vectors, respectively.

The kinetic energy of the shell is given by

$$T(\dot{\delta}) = \frac{1}{2}\int_A [p(\dot{u_0}^2 + \dot{v_0}^2 + \dot{w_0}^2) + I(\dot{\beta_s}^2 + \dot{\beta_\theta}^2)] dA \tag{10}$$

where

$$p = \sum_{i=1}^{N} \int_{z_i}^{z_{i+1}} \rho^i dz, \qquad I = \sum_{i=1}^{N} \int_{z_i}^{z_{i+1}} \rho^i z^2 dz$$

and ρ^i is the mass density of the ith layer. z_i and z_{i+1} are the z coordinate of the inner and outer surfaces of the ith layer. The dot over the variable denotes the partial derivative with respect to time.

Substituting Eqs. (9) and (10) in Lagrange's equation of motion, the governing equation for the shell are obtained as:

$$[\mathbf{M}]\{\ddot{\delta}\} + [C]\{\dot{\delta}\} + [[K] - [K_{\Delta T}] + [K_G] + \frac{1}{2}[N_1(\delta)] + \frac{1}{3}[N_2(\delta)]]\{\delta\} = \{F_M\} + \{F_T\} \tag{11}$$

where $[\mathbf{M}]$ and $[C]$ are the mass and damping matrices, respectively.

The governing Eq. (11) can be employed to study the linear/nonlinear static/dynamic response and eigenvalue analyses by neglecting the appropriate terms as:

Linear Static Analysis:

$$[K]\{\delta\} = \{F_M\} + \{F_T\} \tag{12}$$

Nonlinear Static Analysis:

$$[[K] - [K_{\Delta T}] + [K_G] + \frac{1}{2}[N_1(\delta)] + \frac{1}{3}[N_2(\delta)]]\{\delta\} = \{F_M\} + \{F_T\} \tag{13}$$

Nonlinear Dynamic Analysis:

$$[\mathbf{M}]\{\ddot{\delta}\} + [C]\{\dot{\delta}\} + [[K] - [K_{\Delta T}] + [K_G] + \frac{1}{2}[N_1(\delta)] + \frac{1}{3}[N_2(\delta)]]\{\delta\} = \{F_M\} + \{F_T\} \tag{14}$$

Free Vibration Analysis about Deformed Equilibrium Configuration:

$$[K_t]\{\bar{\delta}\} = \omega^2[\mathbf{M}]\{\bar{\delta}\} \tag{15}$$

where $[K_t] = [K] - [K_{\Delta T}] + [K_G] + [N_1(\delta)] + [N_2(\delta)]$ is the tangent stiffness matrix, $\{\bar{\delta}\}$ is the vector representing the vibration mode shape measured from the deformed equilibrium configuration and ω is the frequency.

Eigenvalue Buckling Analysis:

$$[K]\{\delta\} = \Delta T\{K_G^*\}\{\delta\} \tag{16}$$

where $[K_G^*]$ is the geometric stiffness due to initial state of stress developed because of unit uniform temperature rise and ΔT is the temperature rise.

It may be noted here that for the purpose of evaluating $[K_G^*]$, firstly the static analysis of the shell using Eq. (12) for unit load is carried out. The resulting deformation field is used to calculate the initial state of stress resultants using Eq. (5) and in turn, for evaluating the $[K_G^*]$ matrix.

The description of finite element and its validation can be found in Refs. [15, 16] and for the sake of brevity, is not presented here.

3 Solution methods

3.1 Transient analysis

The Equation(14) for nonlinear dynamic response is solved using the Newmark's numerical integration scheme. If the solution is known at time t and one wishes to obtain the displacements etc., at time $t + \Delta t$, then the equilibrium equations considered at time $t + \Delta t$ are given as

$$[\mathbf{M}]\{\ddot{\delta}\}_{t+\Delta t} + [C]\{\dot{\delta}\}_{t+\Delta t} + [[N(\delta)]\{\delta\}]_{t+\Delta t} = \{F\}_{t+\Delta t} \tag{17}$$

where $\{\ddot{\delta}\}_{t+\Delta t}$, $\{\dot{\delta}\}_{t+\Delta t}$ and $\{\delta\}_{t+\Delta t}$ are the vectors of the nodal accelerations, velocities and displacements at time $t+\Delta t$, respectively; and $\{F\}_{t+\Delta t} = \{F_M\}_{t+\Delta t} + \{F_T\}_{t+\Delta t}$. $\{[N(\delta)]\{\delta\}\}_{t+\Delta t}$ is the internal force vector at time $t+\Delta t$ and is given as

$$\{[N(\delta)]\{\delta\}\}_{t+\Delta t} = \{[[K] - [K_{\Delta T}] + [K_G] + \frac{1}{2}[N_1(\delta)] + \frac{1}{3}[N_2(\delta)]]\{\delta\}\}_{t+\Delta t} \tag{18}$$

In developing equations for the implicit integration, the internal forces $[N(\delta)]\{\delta\}$ at the time $t+\Delta t$ is written in terms of the internal forces at time t, by using the tangent stiffness approach, as

$$\{[N(\delta)]\{\delta\}\}_{t+\Delta t} = \{[N(\delta)]\{\delta\}\}_t + [K_T(\delta)]_t\{\Delta\delta\} \tag{19}$$

where $[K_T(\delta)]_t = [[K] - [K_{\Delta T}] + [K_G] + [N_1] + [N_2]]$ is the tangent stiffness matrix and $\{\Delta\delta\} = \{\delta\}_{t+\Delta t} - \{\delta\}_t$. Substituting Eq. (19) into Eq. (17), one obtains the governing equation at $t+\Delta t$ as

$$[\mathbf{M}]\{\ddot{\delta}\}_{t+\Delta t} + [C]\{\dot{\delta}\}_{t+\Delta t} + [K_T(\delta)]_t\{\Delta\delta\} = \{F\}_{t+\Delta t} - \{[N(\delta)]\{\delta\}\}_t \tag{20}$$

The Eq. (20) is solved using Newmark's numerical integration scheme.

3.2 Nonlinear static analysis

The nonlinear static equilibrium path is traced by solving Eq. (13) using Newton-Raphson iteration procedure coupled with displacement control method [1]. The governing Eq. (13) for the ith load/displacement step, treating ΔT also as unknown variable together with the displacement vector $\{\delta\}$ and using the tangent stiffness approach, can be rewritten as

$$[K_T]\{\delta^i - \delta^{i-1}\} - (\Delta T^i - \Delta T^{i-1})\{\{F_T^*\} + [K_{\Delta T}^*]\{\delta^{i-1}\}\} = \{R^{i-1}\} \tag{21}$$

where

$\{R^{i-1}\} = \{F_M\} + \Delta T^{i-1}\{F_T^*\} - [[K] - \Delta T^{i-1}[K_{\Delta T}^*] + \frac{1}{2}[N_1(\delta^{i-1})] + \frac{1}{3}[N_2(\delta^{i-1})]]\{\delta^{i-1}\}$

$[K_T] = [K] - \Delta T^{i-1}[K_{\Delta T}^*] + [N_1(\delta^{i-1})] + [N_2(\delta^{i-1})]$

Here, $[K_{\Delta T}^*]$ is the thermal geometric stiffness because of unit uniform temperature rise; ΔT^i and δ^i are the temperature rise and displacement vector in the ith step.

In the displacement control method, the qth component of incremental displacement vector $\{\delta^i - \delta^{i-1}\}$ is prescribed. The solution of the remaining displacement and temperature increments is obtained by solving Eq. (21). The degree of freedom q having the highest increment in the previous step is selected as a control parameter except the first step wherein the temperature increment is specified.

The equilibrium iterations are continued for each load/displacement incremental step until the convergence criteria suggested by Bergan and Clough [2] in terms of residual force and iterative displacement increment norms are satisfied within the specific tolerance limit of less than 0.001 percent.

4 Result and discussion

The nonlinear thermoelastic static response, free vibration characteristics and dynamic response of laminated circular cylindrical shells subjected to uniform temperature rise, which may typically be encountered during the cruise flight of a space vehicle, are investigated using the semi-analytical finite element formulation. The buckling mode shapes evaluated from the eigenvalue analysis of a uniformly heated cylindrical shell, having identical support conditions at the two ends, can be classified into longitudinally symmetric and antisymmetric ones for any circumferential wave number (n). The presence of small magnitude initial disturbance in the form of a load spatially proportional to either the longitudinally symmetric or antisymmetric linear buckling mode shape having maximum transverse displacement parameter ($\bar{w}_{0max}/h$) equal to 0.001, unless otherwise is specified, is considered here. The nonlinear prebuckling/postbuckling response is presented as relationship between maximum outward normal displacement parameter (w_{max}/h) versus temperature rise parameter $\lambda_T (= 10^{-6}\Delta T r/h)$. The stability of the equilibrium configurations is investigated from the variation of frequency parameter $\Omega^2 (= \omega^2 r^2 \rho/E_T)$ with temperature rise parameter (λ_T). The positive and negative values of the frequency parameter indicate the stable and unstable equilibrium configurations, respectively.

The material properties used here are
$E_L = 181$ GPa, $E_T = 10.3$ GPa, $G_{LT} = G_{TT} = 7.17$ GPa, $\nu_{LT} = \nu_{TT} = 0.28$, $\alpha_L = 0.02 \times 10^{-6}$ $/^0$C, $\alpha_T = 22.5 \times 10^{-6}/^0$C, $\rho = 1600$ Kg/m^3.

where E, G, ν and α are Young's modulus, shear modulus, Poisson's ratio and coefficient of thermal expansion, respectively. The subscripts L and T are the longitudinal and transverse directions, respectively, with respect to the fibers.

All the layers are of equal thickness and the ply-angle is measured with respect to the meridional axis (s-axis). The first layer is the innermost layer of the shell.

The simply supported immovable boundary conditions of the shells considered here are:
$u_0^0 = u_0^{c1} = u_0^{s1} = u_0^{c2} = u_0^{s2} = u_0^{c3} = u_0^{s3} = u_0^{c4} = u_0^{s4} = v_0^0 = v_0^{c1} = v_0^{s1} = v_0^{c2} = v_0^{s2} = v_0^{c3} = v_0^{s3} = v_0^{c4} = v_0^{s4} = w_0^0 = w_0^{c1} = w_0^{s1} = w_0^{c2} = w_0^{s2} = \beta_\theta^0 = \beta_\theta^{c1} = \beta_\theta^{s1} = \beta_\theta^{c2} = \beta_\theta^{s2} = 0$ at s=0, L

Based on progressive mesh refinement, 48 elements idealization is found to be adequate to model the complete length of the shells.

The nonlinear thermoelastic response and linear vibration characteristics about the deformed configuration of eight-layered cross-ply laminated $(0^0/90^0)_4$ simply supported cylindrical shell (L/r=1, r/h=200, n=9) are shown in Figure 1. The stable part of the equilibrium path is depicted in Figure 1(a) as solid lines and unstable one with dashed lines. The pre-buckling path (Equilibrium path I) is unstable after the bifurcation point. The equilibrium configurations of the shell after bifurcation point follows the path-II or III depending upon whether the small magnitude radial load (considered for initiation of bifurcation in the nonlinear static analysis) is spatially proportional to longitudinally symmetric or antisymmetric linear buckling mode shape. The post-buckled longitudinally symmetric/antisymmetric deformed configuration of the shell, spanning full meridional length and circumferential sector ($2\pi/n$), are depicted in Figure 2

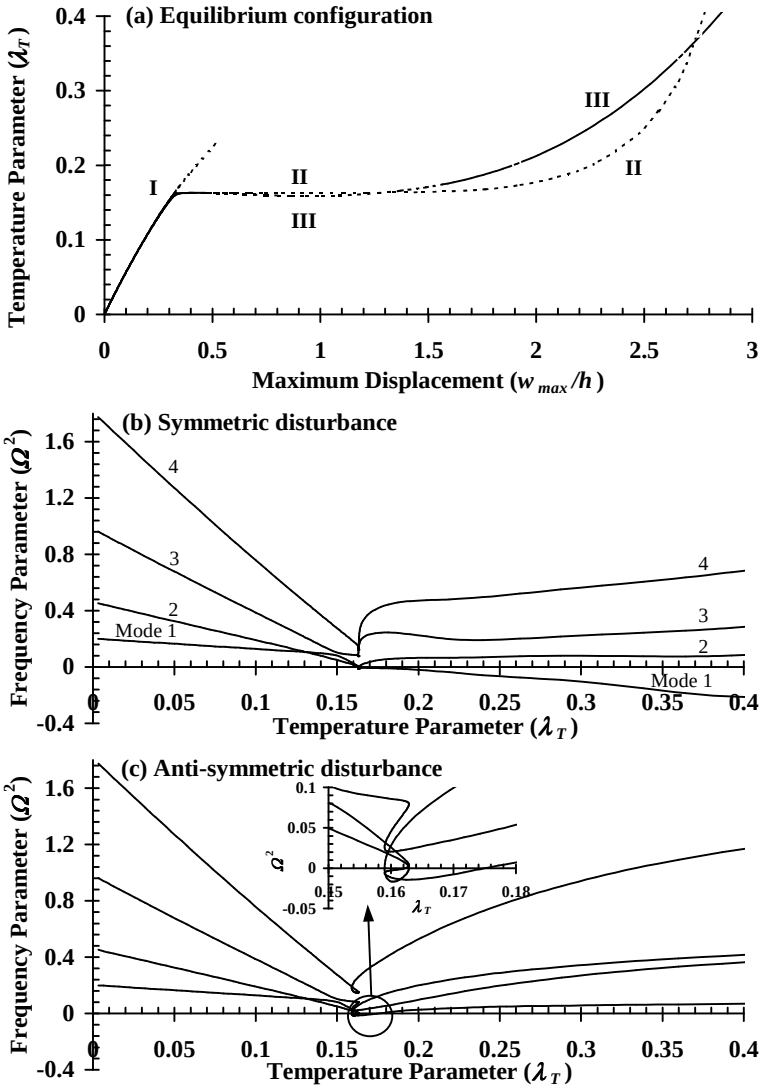

Figure 1: Equilibrium configurations and free vibration frequencies of cross-ply $(0^0/90^0)_4$ laminated heated cylindrical shell ($L/r = 1$, $r/h = 200$, $n = 9$) with longitudinally symmetric and anti-symmetric disturbance.

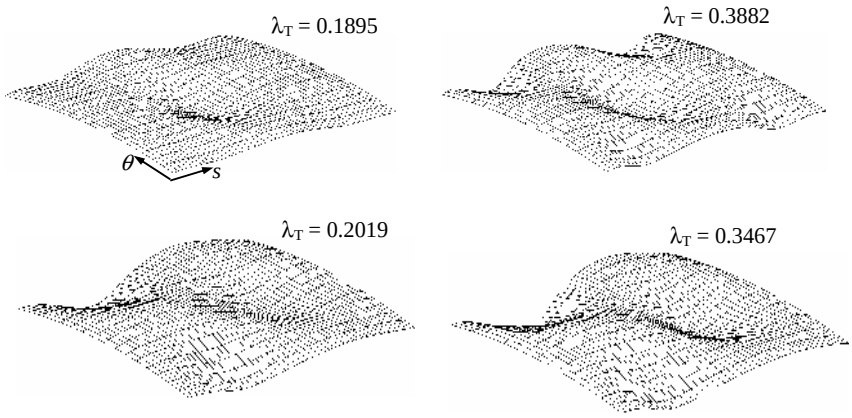

Figure 2: Deformed shape of postbuckled cross-ply laminated $(0^0/90^0)_4$ simply-supported cylindrical shell ($L/r = 1$, $r/h = 200$, $n = 9$): (a) Longitudinally symmetric mode, (b) Longitudinally anti-symmetric mode

for two values of temperature parameter. The frequency parameter variation with temperature presented in Figure 1(b) and 1(c) reveals that the decrease in frequency corresponding to different modes in prebuckling region is independent of type of disturbance (symmetric or antisymmetric). However, the variation of the frequency parameters with temperature significantly depends on the nature (longitudinally symmetric or antisymmetric) of postbuckling equilibrium configuration. The frequency parameter of one mode for longitudinally symmetric postbuckling configuration is negative indicating that the longitudinally symmetric postbuckled configuration is unstable for the entire temperature range considered here. Such behaviour brought out here for circumferentially closed shells is not reported in the vibration characteristics of thermally postbuckled plates/panels [5, 8–14]. The longitudinally antisymmetric postbuckled configuration of the shell is unstable for small range of the temperature parameter as revealed from the frequency parameter variation highlighted in the insert in Figure 1(c). The study carried out considering different circumferential wave numbers (n), L/r and r/h ratios (results are not shown here for the sake of brevity) reveals the similar qualitative behaviour.

To further investigate the stability of symmetric and antisymmetric post-buckled deformed configurations, the dynamic analysis of the shells is carried out incorporating the proportional damping of the form $[C] = \alpha([K] + [M])$. The dynamic response of the heated shell ($\lambda_T = 0.2$) in the presence of longitudinally symmetric disturbance is shown in Figures 3 and 4 for $\alpha = 0.5 \times 10^{-4}$ and 10^{-5}, respectively. It can be observed from Figure 3 and 4 that the shell response grows in the longitudinally symmetric deformation shape and exhibits the oscillations about the mean configuration. The amplitude of these oscillations reduces with the time due

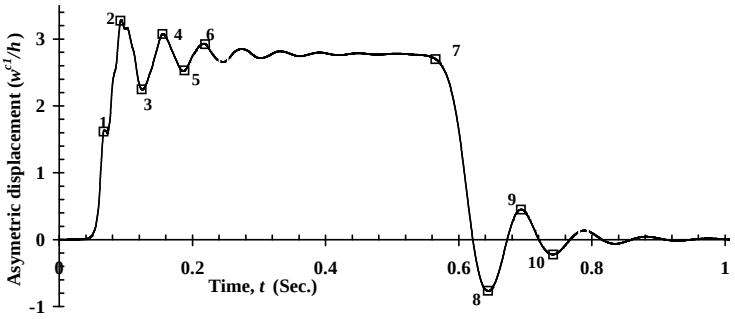

Figure 3: Dynamic response of the heated shell ($\lambda_T = 0.2$) at $s = L/2$ with damping parameter $\alpha = 0.5 \times 10^{-4}$ in the presence of longitudinally symmetric disturbance.

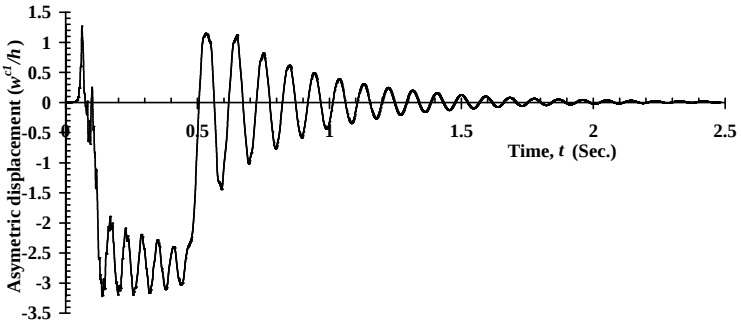

Figure 4: Dynamic response of the heated shell ($\lambda_T = 0.2$) at $s = L/2$ with damping parameter $\alpha = 10^{-5}$ in the presence of longitudinally symmetric disturbance.

to the presence of damping, and when the amplitude of the oscillations is reduced to a certain level depending upon the damping parameter α, the shell response jumps to oscillation about longitudinally antisymmetric mean configuration. It may be noted here that in nonlinear static analysis the longitudinally symmetric disturbance leads to the deformation in the same mode that is predicted as unstable through the eigenvalue analysis. However, in the dynamic analysis, the response of the shell jumps to oscillation about stable configuration even if the assumed initial disturbance is longitudinally symmetric. The deformation shapes of the shell at different time instants (as marked in Figure 3) are shown in Figure 5 depicting the change in the configuration of the shell from longitudinally symmetric to antisymmetric one. The dynamic response shown in Figure 6 for the case of longitudinally antisymmetric disturbance reveals that the shell settles in the same mode without any jump in the response mode shape.

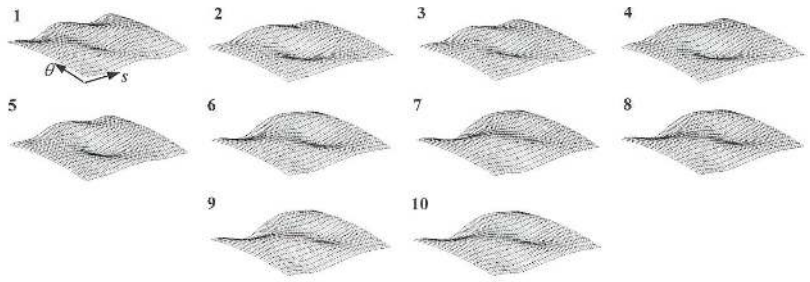

Figure 5: Deformed shapes of shell at different time instants as marked in Figure 3.

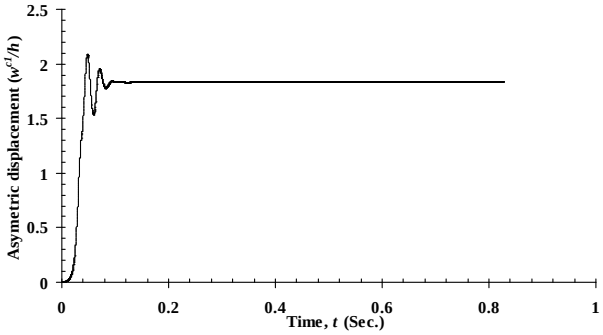

Figure 6: Dynamic response of the heated shell ($\lambda_T = 0.2$) at $s = L/4$ with damping parameter $\alpha = 0.5 \times 10^{-4}$ in the presence of longitudinally antisymmetric disturbance.

Next the forced nonlinear dynamic response analysis of the heated shell is carried out considering λ_T=0.1 (prebuckling region) and 0.2 (postbuckling region). The external radial load is assumed as $q = q_0 \sin(\frac{\pi s}{L}) \cos(n\theta) \sin(\omega_F t)$. The load amplitude q_0 corresponds to a maximum transverse displacement parameter ($\bar{w}_{0max}/h$) in linear static analysis of the shell subjected to only radial load. The steady state response amplitude ($w_0^{c_1}/h$) at $s = L/2$ versus forcing frequency parameter $\Omega_F (= \omega_F\, r \sqrt{\frac{\rho}{E_T}})$ curves, extracted from the time response curves corresponding to different forcing frequencies, are shown in Figure 7. It can be inferred from this Figure that the shell heated in prebuckling region reveals jump phenomenon and forcing frequency corresponding to the jump in the response decreases with the increase in the force magnitude revealing the softening type of nonlinear effect. The response of the shell heated in postbuckling region does not reveal distinct jump. The typical time responses [$w_0^{c_1}/h$ at $s = L/2$ versus non-dimensional time $\tau = \frac{t}{2\pi r} \sqrt{\frac{E_T}{\rho}}$ curves] are shown in Figure 8 for $\lambda_T = 0.1$ and in Figure 9 and 10 for $\lambda_T = 0.2$. The change in the nature of the response pattern is associated with the

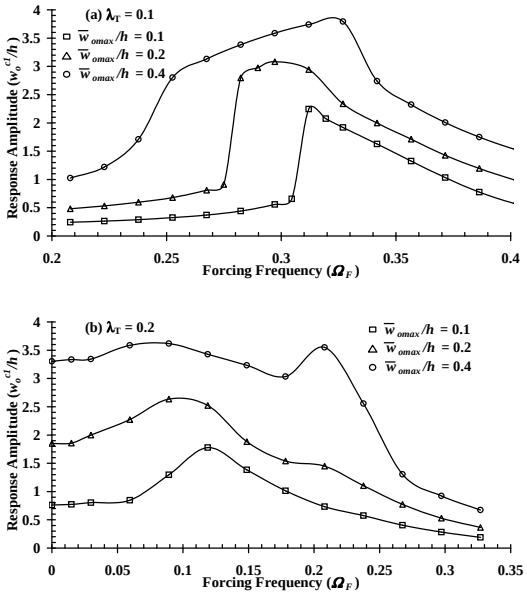

Figure 7: Steady state response amplitude (w_0^{c1}/h) at $s = L/2$ versus forcing frequency parameter Ω_F curves.

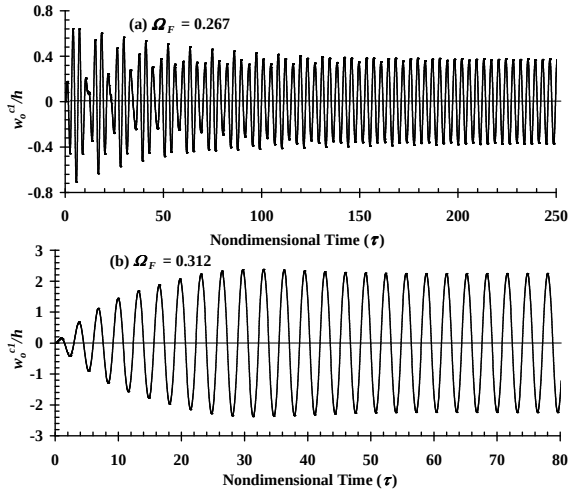

Figure 8: Dynamic response of heated shell ($\lambda_T = 0.1$) at $s = L/2$ with damping parameter $\alpha = 0.5 \times 10^{-4}$ in the presence of radial distributed load ($\bar{w}_{0max}/h = 0.1$).

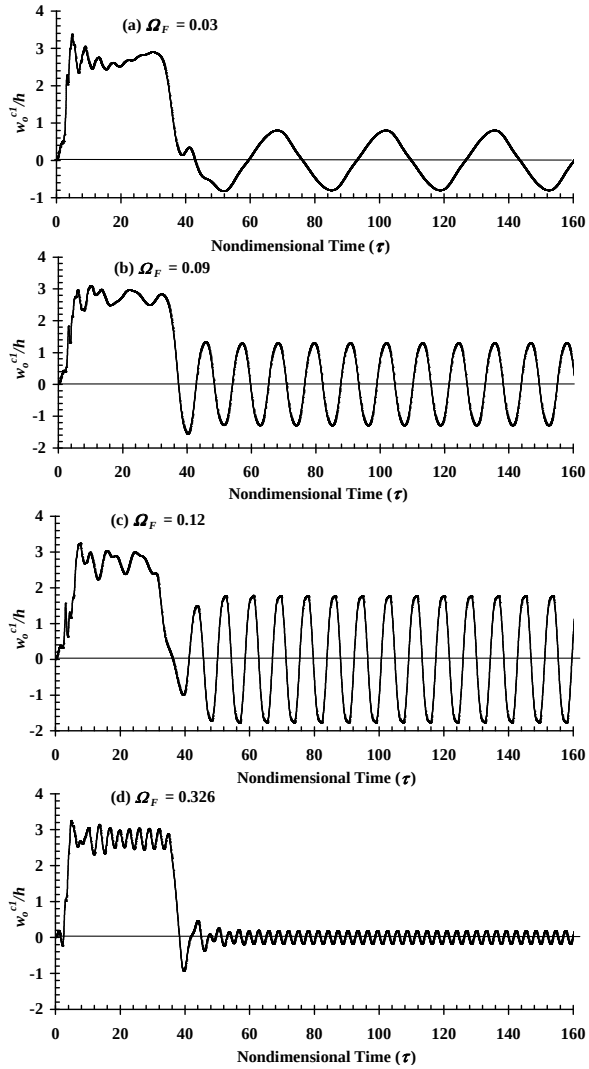

Figure 9: Dynamic response of heated shell ($\lambda_T = 0.2$) at $s = L/2$ with damping parameter $\alpha = 0.5 \times 10^{-4}$ in the presence of radial distributed load ($\bar{w}_{omax}/h = 0.1$).

change of mean equilibrium configuration from longitudinally symmetric to antisymmetric one.

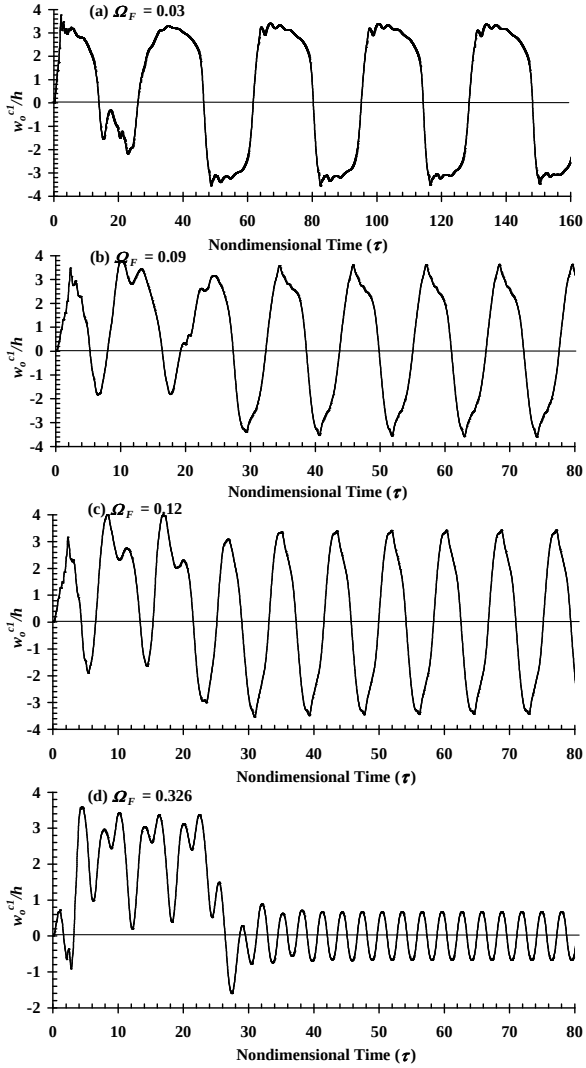

Figure 10: Dynamic response of heated shell ($\lambda_T = 0.2$) at $s = L/2$ with damping parameter $\alpha = 0.5 \times 10^{-4}$ in the presence of radial distributed load ($\bar{w}_{0max}/h = 0.4$).

5 Conclusions

The vibration characteristics of cross-ply laminated heated cylindrical shells are investigated and the stability of their postbuckled equilibrium configurations is studied. The study reveals that the prediction of the postbuckling equilibrium configuration from nonlinear static analysis

depends on the nature (longitudinally symmetric/antisymmetric) of initial disturbance. The longitudinally antisymmetric postbuckled equilibrium configuration is stable whereas the longitudinally symmetric one is unstable for the shell parameters considered here. The dynamic response of the shell reveals shift to stable longitudinally antisymmetric configuration even if the assumed initial disturbance/dynamic radial pressure corresponds to unstable longitudinally symmetric postbuckling configuration. The steady state amplitude - forcing frequency relation depicts jump in the prebuckling region.

References

[1] J.L. Batoz and G. Dhatt. Incremental displacement in nonlinear analysis. *International Journal for Numerical Methods in Engineering*, 14:1262–1267, 1979.

[2] P.G. Bergan and R.W. Clough. Convergence criteria for iterative process. *AIAA Journal*, 10:1107–1108, 1972.

[3] N. Ganesan and R. Kadoli. Buckling and dynamic analysis of piezothermoelastic composite cylindrical shell. *Composite Structures*, 59:45–60, 2003.

[4] N. Ganesan and V. Pradeep. Buckling and vibration of circular cylindrical shells containing hot liquid. *Journal of Sound and Vibration*, 287:845–863, 2005.

[5] J. Girish and L.S. Ramachandra. Thermal postbuckled vibrations of symmetrically laminated composite plates with initial geometric imperfections. *Journal of Sound and Vibration*, 282:1137–1153, 2005.

[6] R.M. Jones. *Mechanics of Composite Materials*. McGraw-Hill, New York, 1975.

[7] H. Kraus. *Thin Elastic Shells*. Wiley, New York, 1976.

[8] D.-M. Lee and I. Lee. Vibration behaviors of thermally postbuckled anisotropic plates using first-order shear deformable plate theory. *Computers and Structures*, 63:371–378, 1997.

[9] L. Librescu and W. Lin. Postbuckling and vibration of shear deformable flat and curved panels on a non-linear elastic foundation. *International Journal of Non-linear Mechanics*, 32:211–225, 1997.

[10] L. Librescu and W. Lin. Non-linear response of laminated plates and shells to thermomechanical loading: Implications of violation of interlaminar shear traction continuity requirement. *International Journal of Solids and Structures*, 36:4111–4147, 1999.

[11] I.-K. Oh and I. Lee. Thermal snapping and vibration characteristics of cylindrical composite panels using layerwise theory. *Composite Structures*, 51:49–61, 2001.

[12] I.K. Oh, J.H. Han, and I. Lee. Postbuckling and vibration characteristics of piezolaminated composite plate subject to thermo-piezoelectric loads. *Journal of Sound and Vibration*, 233:19–40, 2000.

[13] J.-S. Park, J.-H. Kim, and S.-H. Moon. Vibration of thermally post-buckled composite plates embedded with shape memory alloy fibres. *Composite Structures*, 63:179–188, 2004.

[14] J.-S. Park, J.-H. Kim, and S.-H. Moon. Thermal post-buckling and flutter characteristics of composite plates embedded with shape memory alloy fibers. *Composites: Part B*, 36:627–636, 2005.

[15] B.P. Patel, K.K. Shukla, and Y. Nath. Thermal buckling analysis of laminated cross-ply trunctated circular conical shells. *Composite Structures*, 71:101–114, 2005.

[16] B.P. Patel, K.K. Shukla, and Y. Nath. Thermal postbuckling characteristics of laminated conical shells with temperature-dependent material properties. *AIAA Journal*, 43:1380–1388, 2005.

[17] S. Rajasekaran and D.W. Murray. Incremental finite element matrices. *ASCE Journal of the Structural Division*, 99:2423–2438, 1973.